Dof5.6/HCA2, a Dof Transcription Factor Gene, Regulates Interfascicular Cambium Formation and Vascular Tissue Development in *Arabidopsis* [W][OA]

Yong Guo,[a] Genji Qin,[a] Hongya Gu,[a,b] and Li-Jia Qu[a,b,1]

[a] National Laboratory for Protein Engineering and Plant Genetic Engineering, College of Life Sciences, Peking University, Beijing 100871, People's Republic of China

[b] National Plant Gene Research Center (Beijing), Beijing 100101, People's Republic of China

Vascular cambium, a type of lateral meristem, is the source of secondary xylem and secondary phloem, but little is known about the molecular mechanisms of its formation and development. Here, we report the characterization of an *Arabidopsis thaliana* gain-of-function mutant with dramatically increased cambial activity, designated *high cambial activity2* (*hca2*). The *hca2* mutant has no alternative organization of the vascular bundles/fibers in inflorescence stems, due to precocious formation of interfascicular cambium and its subsequent cell division. The phenotype results from elevated expression of *HCA2*, which encodes a nuclear-localized DNA binding with one finger (Dof) transcription factor Dof5.6. *Dof5.6/HCA2* is preferentially expressed in the vasculature of all the organs, particularly in the cambium, phloem, and interfascicular parenchyma cells of inflorescence stems. Dominant-negative analysis further demonstrated that both ubiquitous and in situ repression of HCA2 activity led to disruption of interfascicular cambium formation and development in inflorescence stems. In-depth anatomical analysis showed that *HCA2* promotes interfascicular cambium formation at a very early stage of inflorescence stem development. This report demonstrates that a transcription factor gene, *HCA2,* is involved in regulation of interfascicular cambium formation and vascular tissue development in *Arabidopsis*.

INTRODUCTION

Vascular tissues, either primary or secondary, of higher plants play essential roles in transport of water, nutrients, and signaling molecules and in physical support (Scarpella and Meijer, 2004; Sieburth and Deyholos, 2006). In general, vascular tissue development occurs in a highly ordered and predictable pattern. In plant stems, it involves the formation and regulation of cambium, which consists of fascicular cambium and interfascicular cambium (Lachaud et al., 1999; Helariutta, 2007). Fascicular cambium, initiated from procambium, is present in between the xylem and phloem of a vascular bundle (Larson, 1994). During the formation of interfascicular cambium, interfascicular parenchyma cells located at the edges of the fascicular cambium undergo periclinal asymmetric cell divisions. When the interfascicular cambia originated from two adjacent vascular bundles connect, a continuous ring of vascular cambium is established. A continuous ring of vascular cambium is characteristic of the secondary growth in stems of gymnosperms, woody dicots, and, to a limited extent, some herbaceous dicots (Esau, 1977; Mauseth, 1988).

The formation and activity of vascular cambium have been well documented anatomically and physiologically for the past decade in woody dicots (Iqbal and Ghouse, 1990; Savidge, 1996; Kozlowski and Pallardy, 1997; Lachaud et al., 1999; Mellerowicz et al., 2001). Exploring the molecular mechanisms of vascular cambium formation/development in trees is not an easy task, due to their large sizes, slow growth, and long life cycles. Although much effort has been made in this field, and new systems have been introduced (e.g., *Zinnia elegans* xylogenic culture system and some woody plants), the molecular mechanism of vascular cambium formation/development is far from being clear (Johansson et al., 2003; Motose et al., 2004; Schrader et al., 2004; van Raemdonck et al., 2005; Groover et al., 2006; Hou et al., 2006; Ito et al., 2006; Ko et al., 2006). Fortunately, *Arabidopsis thaliana*, one of the best-known reference plants, has secondary growth in its inflorescence stem, which proves to be an excellent system to dissect further the mechanisms involved in the development of vascular cambium. In addition, the fact that the anatomy of *Arabidopsis* has been well documented makes it easier to identify abnormalities during vascular cambium development (Altamura et al., 2001; Lev-Yadun and Flaishman, 2001; Little et al., 2002; Scarpella and Meijer, 2004).

During the past two decades, some mutants defective in vascular tissue development and a couple of genes involved in this process have been characterized in *Arabidopsis* (Fukuda, 2004; Scarpella and Meijer, 2004; Carlsbecker and Helariutta, 2005; Sieburth and Deyholos, 2006; Baucher et al., 2007). Most of these mutants or transgenic plants display defects in vascular

pattern and secondary cell wall deposition (Hanzawa et al., 1997; Zhong et al., 1997; Zhong and Ye, 1999; Ratcliffe et al., 2000; McConnell et al., 2001; Bonke et al., 2003; Emery et al., 2003; Fisher and Turner, 2007; Mitsuda et al., 2007; Zhong et al., 2007, 2008). Only a few genes have been identified to be related to vascular cambial activity. For instance, *ATHB8*, encoding a class III homeodomain-leucine-zipper-containing (HD-Zip III) transcription factor, is expressed specifically in (pro)cambium cells (Baima et al., 1995). Overexpression of *ATHB8* led to an increase of the vascular cambial activity in inflorescence stems of the transgenic plants, implying that this gene can be used as a marker for vascular cambial activity (Baima et al., 2001). In the *continuous vascular ring1* (*cov1*) mutant, increased vascular tissue in the interfascicular regions of inflorescence stems and loss of the defined vascular bundles are observed, suggesting that *COV1*, encoding a predicted membrane protein, plays a role in the maintenance or the initiation of a defined pattern of vascular bundles (Parker et al., 2003). The mutant *high cambial activity* (*hca*) exhibits high cambial activity and altered vascular patterning, but unfortunately the genetic origin of *hca* is not yet known (Pineau et al., 2005). Due to the small number of the genes identified to be involved in vascular cambium development, the mechanism underlying vascular cambium formation/development remains poorly characterized.

In this study, an *Arabidopsis* mutant with defects in cambium development is identified. The mutant, designated *hca2*, forms a continuous ring of vascular tissues in inflorescence stems, due to very early formation of interfascicular cambium. Our genetic complementation evidence showed that the vascular defects of *hca2* were caused by overexpression of *At5g62940*, which encodes a Dof (DNA binding with one finger) transcription factor Dof5.6. We further found that both ubiquitous and in situ suppression of *Dof5.6/HCA2* with an EAR-motif repression domain resulted in the arrest of interfascicular cambium development. The data from the detailed analysis of *hca2* and chimeric repressor demonstrates that *Dof5.6/HCA2* induces the formation of interfascicular cambium and regulates vascular tissue development.

RESULTS

Isolation of a Mutant with High Cambial Activity *hca2*

In order to identify novel components involved in vascular cambium development in plants, we screened for altered vascular tissues in an *Arabidopsis* activation tagging mutant collection, which was generated using the activation tagging vector pSKI015 as described previously (Qin et al., 2003, 2005). By examining sections of the basal portion of inflorescence stems from 6-week-old plants using light and UV fluorescence microscopy, we identified a mutant in which the organization of vascular tissues was altered. Since the phenotype of this mutant was similar to that of the *hca* mutant with an extraordinarily active vascular cambium (Pineau et al., 2005), we designated it as *hca2*.

To analyze the vascular tissue alterations in more detail, a histological analysis on different organs of *hca2* was conducted. Observation of inflorescence stem cross sections revealed that *hca2* is severely defective both in the patterning and develop-

ment of the vascular bundles. In wild-type plants, six to eight vascular bundles are formed in an ordered and predictable circular pattern in the inflorescence stem, and vascular bundles and interfascicular fibers are separated from the cortex by a single layer of large parenchyma cells (Figure 1A). Fascicular cambium is visible between the xylem and the phloem within each bundle, but interfascicular cambium is hardly detected between vascular bundles (Figure 1B). In the *hca2* mutants, however, the ordered patterning of vascular bundles is replaced by a continuous vascular cambium undergoing periclinal divisions to produce radial files of xylem and phloem. Interfascicular cambium is extensively formed/developed between the vascular bundles, and the area normally occupied by the interfascicular parenchyma cells is replaced by vascular tissues (Figures 1D and 1E). Moreover, in contrast with the wild type (Figure 1C), continuous phloem tissue consisting of several layers of sieve tubes and companion cells encircles the vascular cambium in *hca2* (Figure 1F).

The organization of vascular bundles is also affected in petioles and main veins of leaves. Wild-type petioles and leaf veins exhibit collateral organization of the xylem and phloem, which form distinct layers separated by the (pro)cambium (Figures 1G and 1I). In the petioles and leaf veins of *hca2*, the vascular tissue displays high cambial activity and high phloem proliferation activity (Figures 1H and 1J), similar to the vascular bundles in the inflorescence stem. However, the vascular tissue in the hypocotyls and roots of *hca2* seedlings exhibit no obvious phenotypic alterations (Figures 1K to 1N). These data suggest that the organization of the vascular tissues in the aerial lateral organs is disrupted in the *hca2* mutant.

Cambium and Phloem Specification Genes Are Upregulated, While Xylem Specification Genes Are Downregulated in the *hca2* Mutant

In order to examine the effects of the *hca2* mutation on cambial activity, we used *ATHB8* as a marker for cambial activity and crossed *hca2* mutants with Pro$_{ATHB8}$:*GUS* plants to monitor the expression pattern of *ATHB8* (Baima et al., 1995, 2001) in the *hca2* genetic background. As shown in Figures 2A and 2B, in the basal part of 6-week-old wild-type inflorescence stems, *ATHB8* was expressed primarily in the cambium of each vascular bundle. By contrast, in the basal part of *hca2* inflorescence stems, strong β-glucuronidase (GUS) activity was detected in a continuous ring that is composed of both fascicular and interfascicular cambium, consistent with the histochemical analysis described in Figure 1. The fact that *ATHB8* was upregulated in *hca2* plants suggests that the continuous cambium in *hca2* is highly active.

To examine further the effects of the *hca2* mutation on phloem patterning, we crossed *hca2* mutants with Pro$_{SUC2}$:*GUS* plants to monitor the expression pattern of *SUC2* in the *hca2* background. *SUC2* encodes a companion cell–specific H$^+$-sucrose symporter, and it was reported to be expressed specifically in phloem companion cells (Sauer and Stolz, 1994; Stadler and Sauer, 1996). As shown in Figure 2C, in the basal part of wild-type inflorescence stems, GUS activity was detected in the peripheral vascular bundles, revealing that *SUC2* expression was restricted to the phloem. However, in the basal part of *hca2* inflorescence
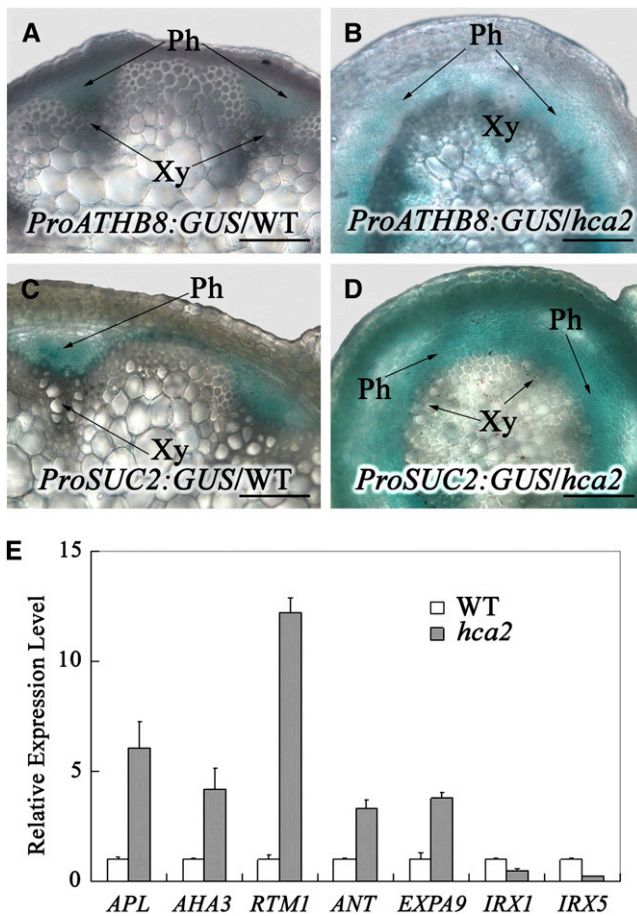
Figure 1. Transverse Sections of Vascular Tissues from 6-Week-Old Plants or 7-d-Old Seedlings of the Wild Type and *hca2*.

(A), **(B)**, **(D)**, and **(E)** Resin-embedded transverse sections of the basal portion of the inflorescence stem from wild-type (**[A]** and **[B]**) and *hca2* (**[D]** and **[E]**) plants stained with Toluidine blue.

(B) and **(D)** Higher magnifications of wild-type and *hca2* vascular tissues, respectively.

(C) and **(F)** Hand-cut transverse sections of the basal portion of the inflorescence stem from wild-type **(C)** and *hca2* **(F)** plants stained with Aniline blue and observed under UV light.

(G) and **(H)** Resin-embedded transverse sections of vascular bundles of petioles from wild-type **(G)** and *hca2* **(H)** plants.

(I) and **(J)** Resin-embedded transverse sections of main veins of rosette leaves from wild-type **(I)** and *hca2* **(J)** plants.

(K) and **(L)** Resin-embedded transverse sections of vascular bundles of hypocotyls from 7-d-old wild-type **(K)** and *hca2* **(L)** seedlings.

(M) and **(N)** Resin-embedded transverse sections of vascular bundles of roots from 7-d-old wild-type **(M)** and *hca2* **(N)** seedlings.

C, cortex; If, interfascicular fiber; Pc, (pro)cambium; Pi, pith; Ph, phloem; S, starch sheath; Vb, vascular bundle; Xy, xylem; Fc, fascicular cambium; Ic, interfascicular cambium. Bars = 200 μm in **(A)**, **(C)**, **(D)**, and **(F)**, 50 μm in **(B)**, **(E)**, and **(G)** to **(J)**, and 20 μm in **(K)** to **(N)**.

stems, strong GUS activity was detected outside the xylem and the GUS staining formed a continuous ring, suggesting that the expression pattern of *SUC2* is completely altered (Figure 2D). These results suggest that phloem patterning was altered in *hca2*.

We further examined the expression of other cambium, phloem, and xylem marker genes (Zhao et al., 2005) in inflorescence stems of the *hca2* mutant by quantitative RT-PCR. These genes included the cambium/xylem marker *EXPA9* (Gray-Mitsumune et al., 2004), cambium marker *ANT* (Schrader et al., 2004), phloem companion cell marker *AHA3* (Dewitt and Sussman, 1995), phloem sieve tube element markers *RTM1* (Chisholm et al., 2001) and *APL* (Bonke et al., 2003), and cellulose synthesis genes *IRX1* and *IRX5*, which are expressed during secondary cell wall development (Taylor et al., 2003). The results

showed that cambium and phloem marker genes were all upregulated, while cellulose synthesis genes were downregulated in the inflorescence stem of the *hca2* mutant (Figure 2E). These results, combined with anatomic analysis of the mutant (Figure 1), suggest that the activity of vascular cambium and the proliferation of phloem are promoted and the number of secondary thickened cells in either xylem or interfascicular fiber regions is reduced in the *hca2* mutant.

The *hca2* Mutation Has Pleiotropic Effects on Plant Morphology

In addition to the vascular tissue defects, the *hca2* mutant also displayed other morphological defects. Like other vascular-altered

Figure 2. The Expression Pattern of Cambium/Phloem/Xylem Biased Genes Is Altered in the *hca2* Mutant.

(A) and **(B)** GUS staining in transverse hand-cut sections from the basal portion of the stem of 6-week-old *Pro_ATHB8*:*GUS* plants in wild-type **(A)** and *hca2* **(B)** backgrounds.

(C) and **(D)** GUS staining in transverse hand-cut sections from the basal portion of the stem of 6-week-old *Pro_SUC2*:*GUS* plants in wild-type **(C)** and *hca2* **(D)** backgrounds.

(E) The expression level of phloem (*APL*, *AHA3*, and *RTM1*)/cambium (*ANT* and *EXPA9*)/xylem (*IRX1* and *IRX5*) biased genes in the inflorescence stems of the wild type and *hca2*. The expression levels of each gene in the wild type are set to 1.0, and error bars represent SD of three biological replicates.

Ph, phloem; Xy, xylem. Bars = 100 μm in **(A)** to **(D)**.

mutants, the inflorescence stem of *hca2* is shorter than that of the wild type, resulting in *hca2* plants being ~30% of the height of the wild type (Figures 3A and 3B). Scanning electron microscopy analysis showed that the epidermal cells were shorter in *hca2* than in the wild type (Figures 3C and 3D), suggesting that the short-internode phenotype is possibly attributable to reduction of individual epidermal cell length. The leaves of *hca2* plants were indistinguishable from those of the wild type when they first emerged. However, at leaf maturity, the petiole and lamina of the *hca2* mutant were smaller than those of the wild type (Figure 3E). Scanning electron microscopy analysis showed that the

average size of epidermal cells was reduced in the mutant leaves (Figures 3F and 3G). These results suggest that the growth of epidermal cells both in inflorescence stems and in leaves is altered in the *hca2* mutant. Moreover, we found that growth of the fifth true leaves in the *hca2* mutant was slower but terminated earlier (Figure 3H). Although the flowers of *hca2* mutants were indistinguishable from those of the wild type, the *hca2* siliques were shorter and the number of seeds per silique reduced (Figure 3I).

The *hca2* Phenotype Is Caused by Overexpression of a Dof Transcription Factor

Because *hca2* is a dominant mutant from an activation tagging mutant collection (Qin et al., 2003), the mutant is probably a gain-of-function mutant caused by a T-DNA insertion. Through thermal asymmetric interlaced (TAIL)-PCR, sequencing and DNA gel blot analysis, we identified a single T-DNA insertion in *hca2* located in the fourth exon of *At5g62950* (Figure 4A). To examine whether the T-DNA insertion cosegregates with the observed phenotypes, we genotyped a T3 population of the *hca2* mutant. Among 399 T3 plants, 82 were wild type without the T-DNA insertion, 98 were homozygous for the T-DNA insertion, and 219 were heterozygous for the T-DNA insertion. All the plants homozygous for the T-DNA insertion displayed severe vascular defects and dwarfism phenotypes, whereas all the plants lacking the T-DNA insertion did not display such phenotypes (data not shown), suggesting that the vascular defects and dwarfism phenotypes are caused by this single T-DNA insertion.

In order to clarify which gene was responsible for the observed phenotypes of *hca2*, we examined expression levels of the six genes that are located within 10 kb upstream and downstream of the T-DNA insertion site. Quantitative RT-PCR analysis showed that expression of *At5g62940* was greatly increased, whereas that of *At5g62950* was completely knocked out (Figure 4B). We first identified a SALK mutant (SALK_117570) in which *At5g62950* was severely knocked down. The morphological appearance of SALK_117570 was similar to that of the wild type (Figures 4C, 4F, and 4I). We next overexpressed *At5g62940*, driven by 4× 35S enhancers, in the transgenic *Arabidopsis*, and found that the overexpressor plants recapitulated the high cambial activity phenotypes (Figures 4C to 4E and 4I). To further confirm that overexpression of *At5g62940* is responsible for the *hca2* phenotypes, we transformed the homozygous *hca2* mutant with an RNA interference (RNAi) construct of *At5g62940* or an overexpression construct of *At5g62950* driven by a cauliflower mosaic virus (CaMV) 35S promoter. In terms of plant height and vascular patterns of the inflorescence stems, 18 out of 21 RNAi transgenic plants exhibited wild-type phenotypes, even in the *hca2* genetic background (Figures 4C, 4G, and 4I). By contrast, the *35S:At5g62950* overexpressor plants in the *hca2* genetic background displayed similar phenotypes to *hca2* (Figures 4C, 4H, and 4I), suggesting that the mutant phenotypes are indeed caused by overexpression of *At5g62940*, rather than by knockout of *At5g62950*. Therefore, *At5g62940* is henceforth referred to as *HCA2*.

HCA2 encodes a putative transcription factor that belongs to the plant-specific Dof transcription factor family in *Arabidopsis*
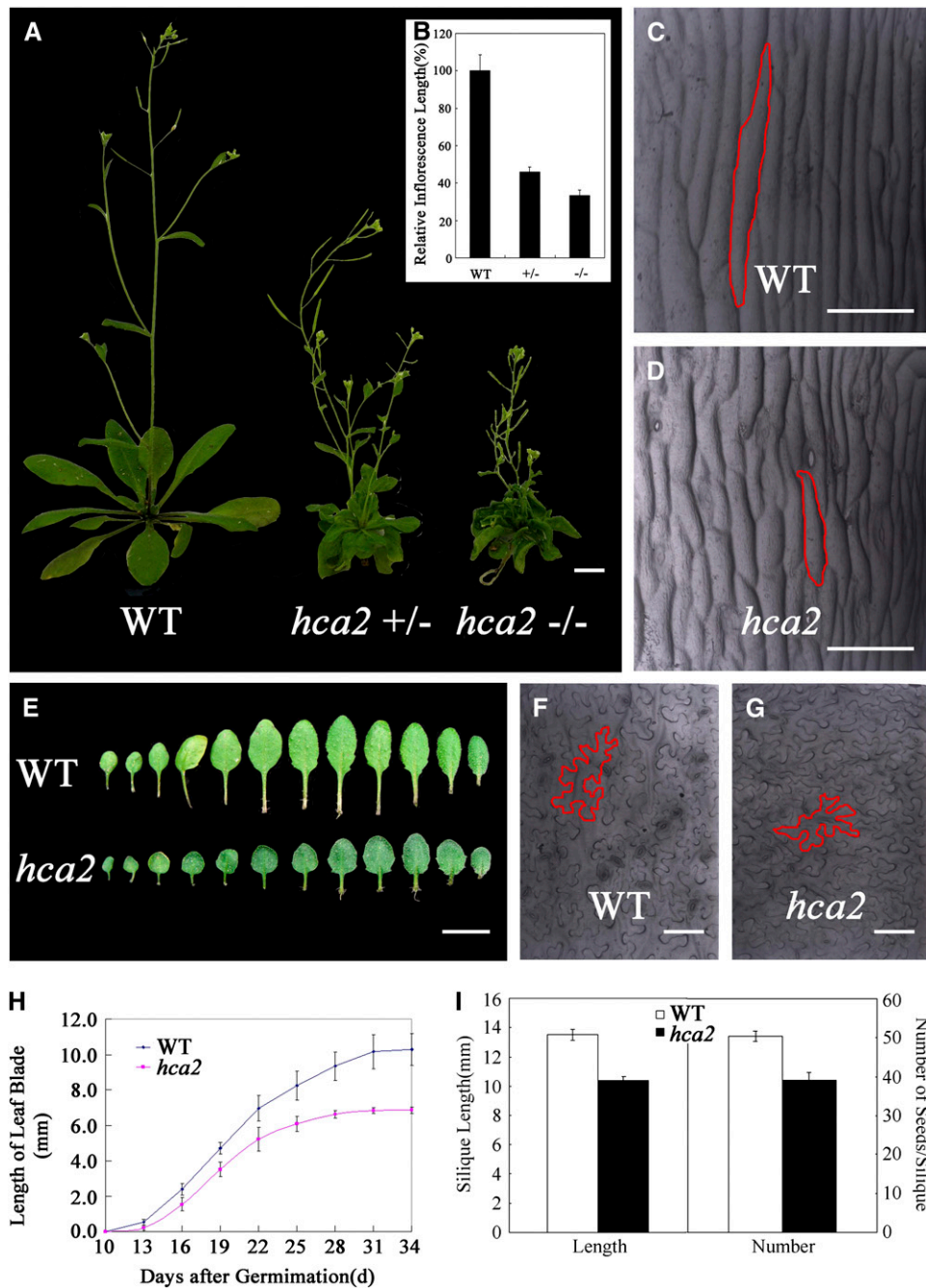
Figure 3. Wild-Type and *hca2* Morphology.

(A) and **(B)** Six-week-old plants grown under long-day conditions **(A)** and final height of the wild-type and *hca2* plants **(B)**. The symbol +/− represents heterozygous mutant, while −/− represents homozygous mutant. The heights of inflorescence stems of at least 15 plants were measured. The average inflorescence stem height of the wild type is set to 100%, and the bars represent SD.

(C) and **(D)** Basal part of inflorescence stems from 6-week-old wild-type **(C)** and *hca2* **(D)** plants visualized by scanning electron micrograph. The red outlines indicate the cell boundary of one single epidermal cell.

(E) Comparison of rosette leaves between wild-type and *hca2* plants. Leaves are arranged from the first leaf at the left to the latest leaf at the right.

(F) and **(G)** Adaxial epidermis of wild-type leaf **(F)** and *hca2* leaf **(G)** visualized by scanning electron micrograph. The red outlines indicate the cell boundary of one single epidermal cell.

(H) The growth rate curves of fifth true leaves from wild-type and *hca2*. At least 15 plants were measured, and the bars represent SD.

(I) Silique length and seed number per silique from wild-type and *hca2* plants. At least 20 siliques were examined and the bars represent SD.

Bars = 1 cm in **(A)**, 1 mm in **(E)**, and 50 μm in **(C)**, **(D)**, **(F)**, and **(G)**.
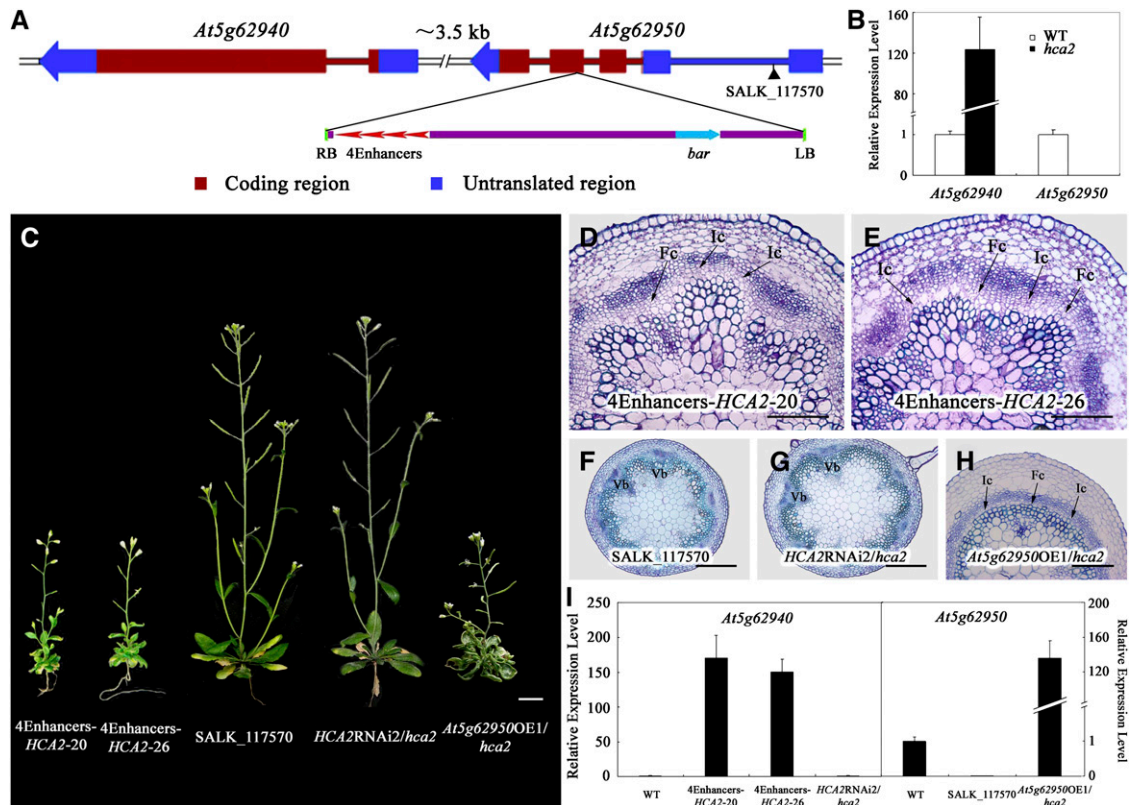
Figure 4. Characterization of the *HCA2* Gene.

(A) Schematic of the genomic region flanking the T-DNA insertion site in *hca2* and SALK_117570. The arrow direction represents the transcriptional orientation of the gene. The four red arrowheads represent the four 35S enhancers from pSKI015. LB, T-DNA left border; *bar*, Basta resistance gene; 4Enhancers, CaMV 35S enhancer tetrad; RB, T-DNA right border.

(B) Expression of *At5g62940* and *At5g62950* in the wild type and the homozygous *hca2* mutant measured by quantitative RT-PCR with *UBQ10* as an internal control. The expression levels of each gene in the wild type are set to 1.0, and error bars represent SD of three biological replicates.

(C) Transgenic plants overexpressing *At5g62940* driven by 4× 35S enhancers (4Enhancers-*HCA2*-20 and -26) show the mutant phenotype, while SALK_117570 did not have any observable phenotype; *hca2* transformed with the *HCA2* RNAi construct or the *At5g62950* overexpression construct (OE1) had wild-type or mutant phenotypes, respectively.

(D) to **(F)** Resin-embedded transverse sections of the basal portion of the stem from transgenic plants line 20 **(D)**, line 26 **(E)**, and SALK_117570 **(F)** stained with Toluidine blue.

(G) and **(H)** *hca2* transformed with the *HCA2* RNAi construct exhibits a wild-type vascular phenotype **(G)**, while *hca2* transformed with the *At5g62950* overexpression construct has the mutant vascular phenotype **(H)**.

(I) Expression levels of *At5g62940* and *At5g62950* in transgenic plants and SALK_117570 were measured with quantitative RT-PCR. The expression levels of each gene in the wild type are set to 1.0, and error bars represent SD of three biological replicates.

Fc, fascicular cambium; Ic, interfascicular cambium; Vb, vascular bundle. Bars = 1 cm in **(C)**, 100 μm in **(D)** and **(E)**, and 200 μm in **(F)** to **(H)**.

and is designated *Dof5.6* based on its chromosomal position (Yanagisawa, 2002). There are 36 *Dof* gene family members found in the *Arabidopsis* genome, three of which, *At2g28510*, *At3g45610*, and *At5g60200*, clustered in the same clade with *Dof5.6/HCA2* in the phylogenetic tree (Lijavetzky et al., 2003; Yang et al., 2006).

HCA2 Is Localized to the Nucleus and Has Transactivating Activity in Yeast

To determine the subcellular localization of HCA2, we transformed a yellow fluorescent protein (YFP)-HCA2 fusion protein construct, driven by a CaMV 35S promoter, into wild-type *Arabidopsis*. In the wild type, no or weak fluorescence was detected (Figure 5A), whereas YFP fluorescence was visible both in the cytoplasm and nucleus of *35S:YFP* transgenic plants (Figure 5B). In addition, strong YFP fluorescence was detected in the nucleus of trichomes of the *35S:YFP-HCA2* transgenic plants (Figure 5C), consistent with a role for HCA2 as a transcription factor.

Because the Dof DNA binding domain is conserved among Dof transcription factors, the C-terminal sequence of HCA2 might be functionally important for transcriptional activity. To elucidate which region was responsible for transactivation activity, we
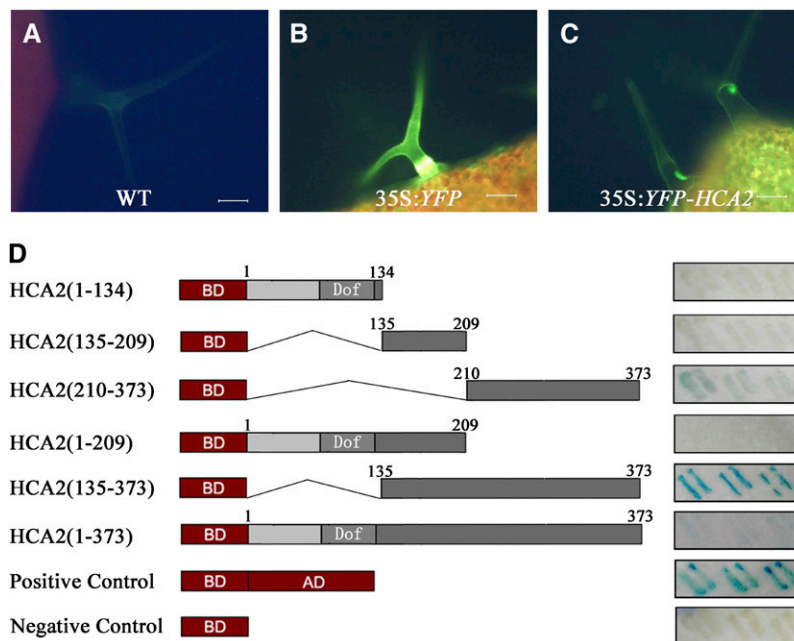
Figure 5. Subcellular Localization of YFP-HCA2 Protein and Transactivation Activity of HCA2.

(A) Trichome of leaf from wild-type plant visualized under the fluorescence microscope.
(B) Trichome of leaf from 35S:*YFP* plant visualized under the fluorescence microscope.
(C) Trichome of leaf from 35S:*YFP-HCA2* plant visualized under the fluorescence microscope.
(D) Transactivation activity of HCA2 in yeast. The full-length open reading frame of *HCA2* and its deletion constructs are illustrated schematically. The Dof domain is labeled. The panels to the right show yeast transformed with the indicated constructs. Blue color represents transactivation.
Bars = 200 μm in **(A)** to **(C)**.

generated a series of deletions in HCA2 and fused them to the GAL4 DNA binding domain (Figure 5D) before they were co-transformed into yeast with a reporter vector (Li et al., 2006). The results showed that the C-terminal region without the Dof domain (i.e., the region 135 to 373 amino acids) displayed the highest transactivation activity, whereas the extreme C-terminal region (210 to 373 amino acids) showed much weaker activity (Figure 5D). No GUS activity was detected for the negative control and all the constructs containing the Dof motif sequence, including the full-length HCA2 construct (Figure 5D). These results suggest that the C-terminal region (135 to 373 amino acids) is responsible for the transactivation activity and that the Dof domain somehow hampers transactivation activity.

HCA2 Is Predominantly Expressed in Cambium, Phloem, and Interfascicular Parenchyma Cells

We first adopted quantitative RT-PCR to examine the expression pattern of *HCA2* in different *Arabidopsis* tissues and organs. *HCA2* was ubiquitously expressed in 2-week-old seedlings and in all organs of 6-week-old plants, at a similar expression level (Figure 6A). To investigate further the expression of *HCA2*, ~2 kb of the *HCA2* promoter region was fused to the *Escherichia coli* GUS reporter gene and transformed into *Arabidopsis*. As shown in Figures 6B to 6D, GUS activity was observed in the vascular tissues and pericycle of primary roots. Similarly, strong GUS

activity was detected in the vasculature of the cotyledons, rosette leaves, and cauline leaves (Figures 6E to 6G). Strong GUS activity was also observed in vasculature of petals, the stigma, and stamen filaments, whereas weaker staining was detectable in anthers and carpels (Figure 6H). Cross sections of inflorescence stems also revealed strong GUS activity in the vasculature, particularly in cambium, phloem, and interfascicular parenchyma cells (Figures 6I and 6J). This is consistent with the previously reported microarray result that *HCA2* exhibits a cambium/phloem tissue-biased expression pattern in root hypo-cotyls of *Arabidopsis* (Zhao et al., 2005). Taken together, the expression of *HCA2* is concentrated mainly in the vascular tissues, from the seedling stage to the mature plant.

Both Ubiquitous and Localized Expression of Chimeric *HCA2* Repressors Induced Vascular Tissue Defects

In order to investigate the function of *HCA2*, we first examined the phenotypes of the *HCA2* mutants requested from SALK (SALK008810 and CS853250) and found no obvious vascular patterning phenotype, since the expression levels of *HCA2* is not altered (see Supplemental Figure 1 online). It has been reported that there are three Dof protein members clustered (*At2g28510*, *At3g45610*, and *At5g60200*) in the same clade with *HCA2* in the phylogenetic tree (Lijavetzky et al., 2003). In the ABRC database, no loss-of-function mutant is available for the other two genes
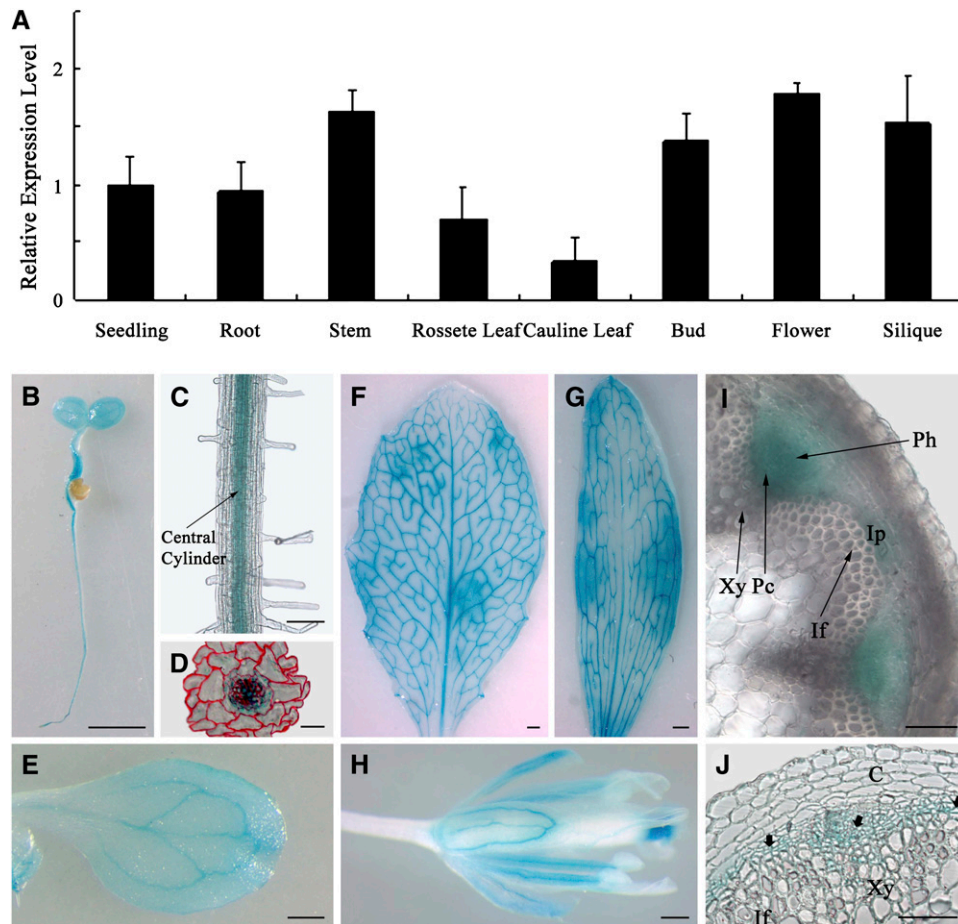
Figure 6. Spatial Expression Pattern of *HCA2.*

(A) Analysis of *HCA2* expression level in different organs by quantitative RT-PCR. The expression level in the seedling is set to 1.0, and error bars represent SD of three biological replicates. Wild-type plants were transformed with the *Pro_HCA2*:*GUS* fusion construct.
(B) GUS-stained 5-d-old seedling growing on Murashige and Skoog solid medium.
(C) Longitudinal view of GUS-stained root from 5-d-old seedling.
(D) GUS and Safranin (red color)-stained 7-μm cross section of the maturation zone of primary roots.
(E) GUS-stained cotyledon of 13-d-old seedling.
(F) to **(H)** GUS-stained rosette leaf **(F)**, cauline leaf **(G)**, and flower **(H)** of a 6-week-old plant.
(I) and **(J)** Transverse sections of an inflorescence stem. Note the GUS staining in cambium, phloem, and interfascicular parenchyma cells. Bold arrows in **(J)** indicate the GUS-stained cells.
C, cortex; If, interfascicular fiber; Pc, (pro)cambium; Ph, phloem; Xy, xylem; Ip, interfascicular parenchyma cell. Bars = 1 mm in **(B)** and **(E)** to **(H)**, 100 μm in **(C)**, 20 μm in **(D)**, and 50 μm **(I)** and **(J)**.

(*At2g28510* and *At3g45610*). There are three mutants available for *At5g60200*, but, when we examined them by quantitative RT-PCR, none of the three lines exhibited reduced expression of *At5g60200* (see Supplemental Figure 1 online), possibly due to insertion sites that are in the 3′-untranslated regions. Therefore, we generated RNAi transgenic plants for each of the four genes. Phenotypic analysis showed that, although the corresponding gene expression was remarkably reduced, none of the RNAi transgenic plants of each gene (including *HCA2*) had obvious phenotypes (see Supplemental Figure 2 online). Neither did some lines in which two genes were simultaneously knocked down (see Supplemental Figure 3 online). We further crossed an

RNAi line of *HCA2*, HCA2RNAi2, with that of *At3g45610*, At3g45610RNAi7, in each of which the expression of the corresponding gene was greatly reduced (see Supplemental Figures 2 and 3 online). The double RNAi plants, in which the expressions of the four genes were all downregulated to some extent, still looked normal in terms of vascular development (see Supplemental Figure 4 online). The lack of evident vascular phenotypes in single and double RNAi transgenic plants could possibly be due to a functional redundancy between *HCA2* and other homologous Dof gene members.

Therefore, in order to gain more insight into the role of *HCA2* in vascular cambium development, we adopted chimeric repressor

silencing technology to, in the transgenic plants, convert HCA2 into a dominant-negative regulator by fusing it with the EAR-motif repression domain driven by a CaMV 35S promoter or the *HCA2* promoter itself (Hiratsu et al., 2003, 2004). Multiple transgenic plants were generated for the two constructs, and two lines for each, *35S:HCA2SRDX3* and *35S:HCA2SRDX5* for the ubiquitous chimeric repressor and *Pro_{HCA2}:HCA2SRDX5* and *Pro_{HCA2}: HCA2SRDX21* for the in situ chimeric repressor, with slightly differing severity of the phenotypes were chosen for further analysis. As shown in Figure 7A, the hypocotyls of both *35S: HCA2SRDX* and *Pro_{HCA2}:HCA2SRDX* seedlings were longer than those of wild-type seedlings, and the cotyledons curled downward. In addition, the petioles and leaf laminas of transgenic plants were longer and narrower compared with those of wild-type plants (Figures 7B and 7C). Quantitative RT-PCR analysis showed that, whereas expression of the endogenous *HCA2* gene remained at the same level, the expression level of *HCA2SRDX* was positively correlated with the severity of phenotypes in the *35S:HCA2SRDX* transgenic plants (Figure 7D). This suggests that the phenotypes of the *35S:HCA2SRDX* plants are not likely due to cosuppression effects on *HCA2*. In the *Pro_{HCA2}:HCA2SRDX* plants, we did not detect much difference in the expression levels of either endogenous *HCA2* or *HCA2SRDX*, consistent with the very similar phenotypes observed in these two lines (Figure 7D).

Regarding vascular tissues in the basal part of the inflorescence stems, although no/very little interfascicular cambium is formed in 6-week-old wild-type plants, interfascicular cambium is evidently produced by periclinal and oblique divisions in interfascicular regions after the growth of two more weeks, initiating at the edges of the fascicular cambium and spreading later (Figure 7E, left panel). However, in 8-week-old *35S: HCA2SRDX* transgenic plants, almost no dividing interfascicular parenchyma cells could be observed between the vascular bundles (Figure 7E, middle and right panels), suggesting that interfascicular cambium is not initiated in inflorescence stems of the constitutive chimeric repressor plants. In the 8-week-old *Pro_{HCA2}:HCA2SRDX* transgenic plants, similar phenotypes were observed in terms of interfascicular cambium production compared with *35S:HCA2SRDX* transgenic plants (Figure 7F), confirming that in situ chimeric repression of *HCA2* also led to inhibition of the initiation of interfascicular cambium in inflorescence stems and that the vascular phenotypes observed in the *35S:HCA2SRDX* plants are due to the localized suppression of *HCA2.*

HCA2 Regulates Interfascicular Cambium Formation at a Very Early Stage during Inflorescence Stem Development

In order to study further the role of *HCA2* during vascular cambium development, cross sections were taken at subapical and middle positions along the inflorescence stems of 6-week-old wild-type, *hca2*, *35S:HCA2SRDX5*, and *Pro_{HCA2}:HCA2SRDX5* transgenic plants for microscopy observation. The results showed that abnormal vascular tissues were observed not only at the basal part of the *hca2*, *35S:HCA2SRDX5*, and *Pro_{HCA2}: HCA2SRDX5* inflorescence stems but also at the subapical and middle positions. In the wild-type plants, the pattern of vascular

bundles is clearly defined at the subapical position of inflorescence stems, and the triangular-shaped vascular bundles alternate with interfascicular fibers at the middle position (Figures 8A and 8E). In the *hca2* mutant, however, additional differentiation of vascular tissues was already evident in the region immediately below the apical meristem, which was typically occupied by interfascicular parenchyma cells in the wild type (Figure 8B). Interfascicular cambium, originated from parenchyma cells after periclinal division, was present in between enlarged vascular bundles, and additional differentiation of the cells directly adjacent to the developing vascular bundles occurred (Figure 8B). At the middle position of *hca2* inflorescence stems, a continuous ring of vascular cambium was already present (Figure 8F). In the inflorescence stems of both *35S:HCA2SRDX5* and *Pro_{HCA2}: HCA2SRDX5* plants, the anatomy of vascular tissues at the subapical position was very similar to that of the control (Figures 8C and 8D), while at the middle position, no/fewer interfascicular fibers were present between vascular bundles (Figures 8G and 8H), which is consistent with the cross section results at the basal position. These histological data suggest that *HCA2* might regulate vascular cambium formation/development at a very early stage.

Because vascular tissues develop in tight accordance with inflorescence stem development in *Arabidopsis*, different positions on the inflorescence stem will represent a different developmental stage at which the vascular tissues stay. In order to investigate further which developmental stage during interfascicular cambium formation at the subapical position is regulated by *HCA2*, we took a series of cross sections at positions that are 200, 500, 1000, 1500, and 2000 μm, respectively, away from the inflorescence stem apex of 6-week-old wild-type, *hca2*, *35S: HCA2SRDX5*, and *Pro_{HCA2}:HCA2SRDX5* repressor plants for examination under microscopes. The results showed that, in the wild type, vascular bundles, separated by interfascicular parenchyma cells, were already in shape, whereas groups of meristematic cells were still present in the interfascicular regions at the position of ~200 μm apart from the apex (Figure 9A). At the position 500 μm from the apex, vascular bundles started to display differential localization for primary phloem and xylem (i.e., the phloem was located outside the xylem), and very little cell division was observed in the interfascicular regions (Figure 9E). At the 1000 and 1500 μm positions, the primary phloem and primary xylem had differentiated, and a small group of procambium cells, arranged in a radial series, was located between phloem and xylem. The anatomical characteristics of interfascicular parenchyma cells were similar to those of the cells at the 500 μm position (Figures 9I and 9M). At the position ~2000 μm from the apex, different cell types in vascular bundles continued differentiating, with no cell differentiation in the interfascicular regions (Figure 9Q). In the *hca2* mutant, whereas there was no vascular bundle difference observed at the 200 μm position (Figure 9B), interfascicular parenchyma cells located at the edges of the existing vascular bundles had already started to undergo periclinal cell divisions at the 500 μm position, suggesting the initiation of interfascicular cambium formation (Figure 9F). The more distant from the apex (i.e., at 1000 and 1500 μm positions), the more interfascicular parenchyma cell divisions were observed (Figures 9J and 9N). Furthermore, an
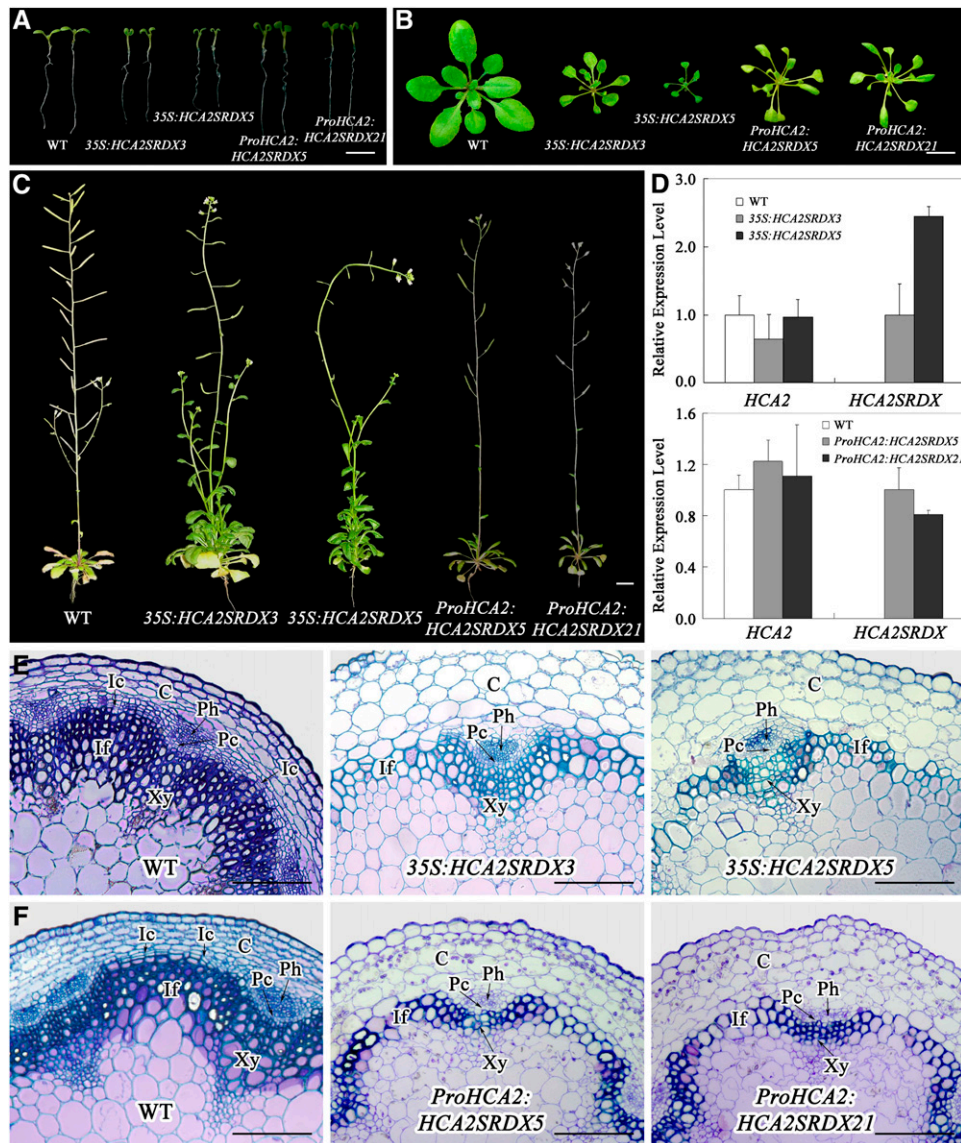
Figure 7. Both Ubiquitous and in Situ Expression of the Chimeric *HCA2* Repressors Alter Vascular Patterning in *Arabidopsis*.

(A) Seven-day-old wild-type, *35S:HCA2SRDX*, and *Pro_HCA2:HCA2SRDX* plants are shown. Two independent lines are shown for each transgene.
(B) Four-week-old wild-type, *35S:HCA2SRDX*, and *Pro_HCA2:HCA2SRDX* plants are shown.
(C) Eight-week-old wild-type, *35S:HCA2SRDX*, and *Pro_HCA2:HCA2SRDX* plants are shown.
(D) The expressions of the *HCA2SRDX* transgene and the endogenous *HCA2* gene in *35S:HCA2SRDX* or *Pro_HCA2:HCA2SRDX* plants were examined by quantitative RT-PCR analysis. The expression levels of *HCA2* in the wild type and *HCA2SRDX* in *35S:HCA2SRDX3* or *Pro_HCA2:HCA2SRDX5* are set to 1.0, and error bars represent SD of three biological replicates.
(E) Resin-embedded transverse sections of the basal part of the stem from wild-type and two lines of *35S:HCA2SRDX* plants.
(F) Resin-embedded transverse sections of the basal part of the stem from wild-type and two lines of *Pro_HCA2:HCA2SRDX* plants.
C, cortex; If, interfascicular fiber; Pc, (pro)cambium; Ph, phloem; Xy, xylem; Fc, fascicular cambium; Ic, interfascicular cambium. Bars = 0.5 cm in **(A)**, 1 cm in **(B)** and **(C)**, and 100 μm **(E)** and **(F)**.

almost-completed continuous vascular cambium ring had already been formed at the 2000 μm position (Figure 9R). These observations suggest that the continuous ring of vascular cambium in *hca2* is formed through the earlier activation of periclinal cell division activity in the interfascicular region. Different than the

hca2 mutant, almost no obvious vascular development differences could be observed compared with the wild type at corresponding positions in *35S:HCA2SRDX5* and *Pro_HCA2: HCA2SRDX5* transgenic plants (Figures 9C, 9D, 9G, 9H, 9K, 9L, 9O, 9P, 9S, and 9T). Taken together, these results suggest
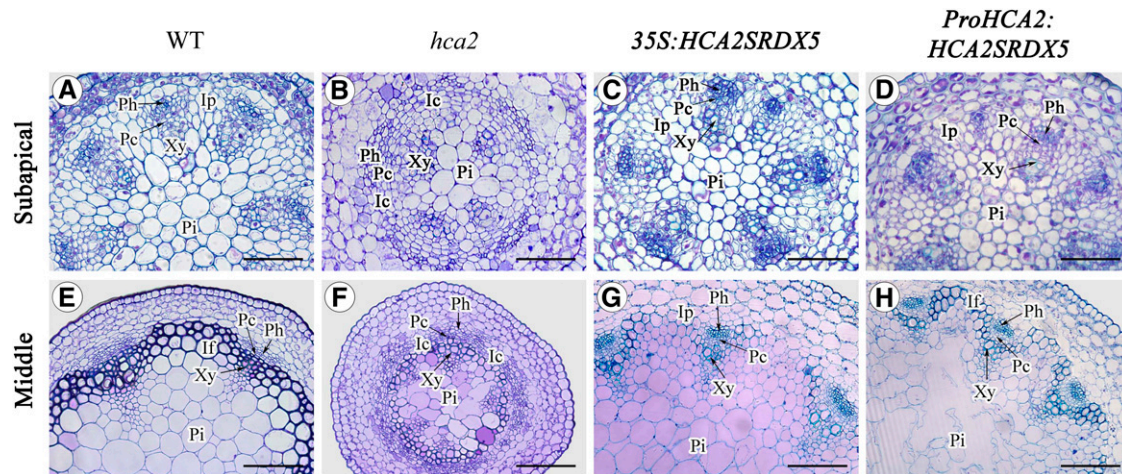
Figure 8. Vascular Tissue Development of the Inflorescence Stems in Wild-Type, *hca2*, *35S:HCA2SRDX5*, and *Pro_HCA2:HCA2SRDX5* Plants.

(A) to **(D)** Resin-embedded transverse sections of the subapical part of the inflorescence stem from wild-type **(A)**, *hca2* **(B)**, *35S:HCA2SRDX5* **(C)**, and *Pro_HCA2:HCA2SRDX5* **(D)** plants.
(E) to **(H)** Resin-embedded transverse sections of the middle part of the inflorescence stem from wild-type **(E)**, *hca2* **(F)**, *35S:HCA2SRDX5* **(G)**, and *Pro_HCA2:HCA2SRDX5* **(H)** plants.
If, interfascicular fiber; Pc, (pro)cambium; Ph, phloem; Xy, xylem; Ic, interfascicular cambium; Ip, interfascicular parenchyma cell; Pi, pith. Bars = 50 μm in **(A)** to **(D)** and 100 μm in **(E)** to **(H)**.

that *HCA2* regulates interfascicular cambium formation possibly by affecting periclinal division activity of the interfascicular parenchyma cells after vascular bundle formation.

DISCUSSION

In this study, we provide evidence that a Dof transcription factor gene *Dof5.6/HCA2* plays an important role in the regulation of vascular tissue development. In particular, our data suggest that *HCA2* is likely to act as a positive regulator to promote initiation of the interfascicular cambium from interfascicular parenchyma cells.

We found that the inflorescence stem of wild-type *Arabidopsis* showed almost no/weak formation of interfascicular cambium after 6 weeks of growth, and six to eight vascular bundles were arranged alternatively by interfascicular parenchyma cells in the basal region. In the *hca2* mutant, however, a number of interfascicular parenchyma cells were found to start periclinal division and subsequently to form interfascicular cambium. Therefore, the increased production of interfascicular cambium in the *hca2* mutant could be attributed to a stimulation of proliferation and dedifferentiation of interfascicular parenchyma cells. This process occurred at a very early stage during vascular tissue development, possibly promoted by *HCA2* via increasing periclinal division activity of the interfascicular parenchyma cells after vascular bundle formation (Figure 9). On the contrary, the formation of the interfascicular cambium was found to be inhibited in the basal part of the transgenic plants either ubiquitously or in situ expressing the *HCA2* chimeric repressor after 8 weeks of growth (Figure 7), when in the wild-type the interfascicular cambium had been formed. These results together support the conclusion that HCA2 may promote the formation of interfascicular cambium in *Arabidopsis* inflorescence stems.

Dof transcription factors are a family of plant-specific transcription factors, possessing nearly identical Dof zinc finger domains that are required for binding to the sequence 5′-(T/A)AAAG-3′ in promoters (Plesch et al., 2001; Yanagisawa, 2002, 2004). Different Dof transcription factors may form homo- and/or heterodimeric complexes in a given cell type and have various functions, acting as positive or negative regulators of target genes. The Dof domain-containing proteins are reported to be involved in many different plant-specific physiological processes, including light-dependent gene regulation in maize (*Zea mays*; Yanagisawa and Sheen, 1998), activation of storage protein genes in maize and barley (*Hordeum vulgare*; Vicente-Carbajosa et al., 1997; Mena et al., 1998), and regulation of seed germination, defense response, phytochrome signaling, and secondary metabolism in *Arabidopsis* (Papi et al., 2000; Gualberti et al., 2002; Park et al., 2003; Skirycz et al., 2006, 2007). Recently, two Dof transcription factors genes, i.e., *Dof2.4* and *Dof5.8*, were reported to be expressed specifically in cells at the early stage of vascular tissue development either in embryos, young leaves, roots, or flower buds, implying that these two Dof proteins may be involved in vascular tissue development (Konishi and Yanagisawa, 2007). *Dof5.6/HCA2* encodes a protein with transactivating activity that is localized to the nucleus, consistent with the role as a Dof transcription factor (Figure 5). From the data presented in this study, *HCA2* plays an important role in vascular cambium development in *Arabidopsis*. Although HCA2 shares high sequence identity with Dof2.4 and Dof5.8 in the Dof domain, the similarity among the sequences outside the Dof domains is low (data not shown), and these three proteins are not clustered in the same clade in the phylogenetic tree (Lijavetzky et al., 2003),
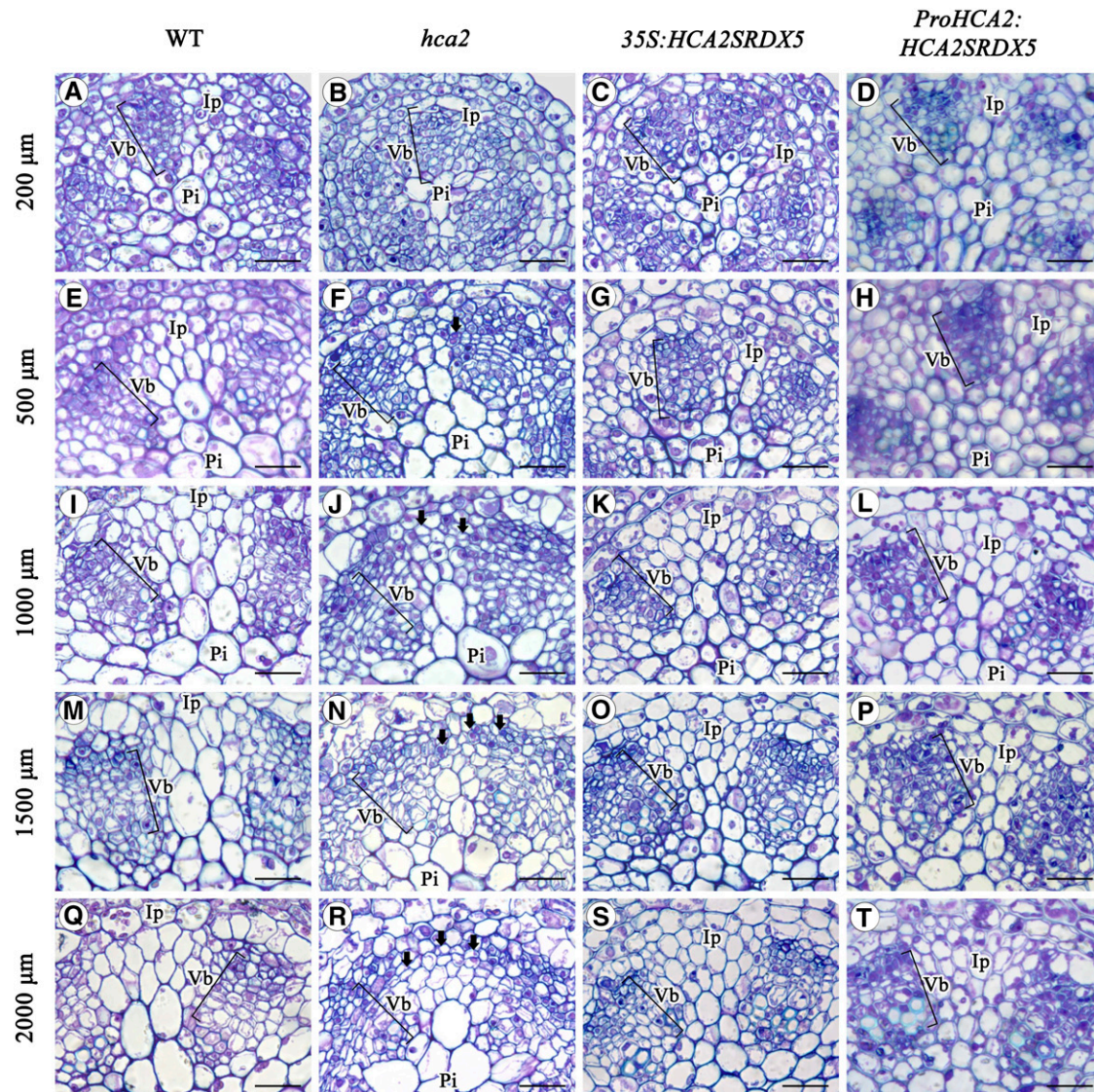
Figure 9. Vascular Tissue Development at the Subapical Part of the Inflorescence Stems in 6-Week-Old Wild-Type, *hca2*, *35S:HCA2SRDX5*, and *Pro_HCA2_:HCA2SRDX5* Plants.

Serial cross sections of the subapical part of the inflorescence stems from the wild type (**[A]**, **[E]**, **[I]**, **[M]**, and **[Q]**), *hca2* (**[B]**, **[F]**, **[J]**, **[N]**, and **[R]**), *35S: HCA2SRDX5* (**[C]**, **[G]**, **[K]**, **[O]**, and **[S]**), and *Pro_HCA2_:HCA2SRDX5* (**[D]**, **[H]**, **[L]**, **[P]**, and **[T]**) were taken, and the images 200 μm (**[A]** to **[D]**), 500 μm (**[E]** to **[H]**), 1000 μm (**[I]** to **[L]**), 1500 μm (**[M]** to **[P]**), and 2000 μm (**[Q]** to **[T]**) from apex are shown. Bold arrows in this diagram indicate interfascicular parenchyma cell divisions. Ip, interfascicular parenchyma cell; Vb, vascular bundle; Pi, pith. Bars = 20 μm.

suggesting a functional divergence among these three different Dof members. Our results from this study showed that three more Dof members, in the same clade with HCA2, are likely to be functionally redundant in regulating vascular tissue development (see Supplemental Figures 2 to 4 online). The existence of multiple Dof genes in the *Arabidopsis* genome that are potentially vascular tissue development associated suggests that a complicated regulation network is possibly adopted in the regulation of vascular tissue development. This may account for the long but not very successful efforts to clone genes controlling vascu-

lar tissue development by traditional mutant screening. It will be interesting and helpful to determine the association of these Dof genes with vascular tissue development by overexpressing them in transgenic plants in the future.

A continuous ring of vascular tissues in the stems has also been reported in two *Arabidopsis* mutants, *cov1* and *hca* (Parker et al., 2003; Pineau et al., 2005). The COV1 protein is a putative integral membrane protein, and the *COV1* gene is likely to be involved in negative regulation of vascular tissue differentiation in the developing stem (Parker et al., 2003). The *hca* mutant
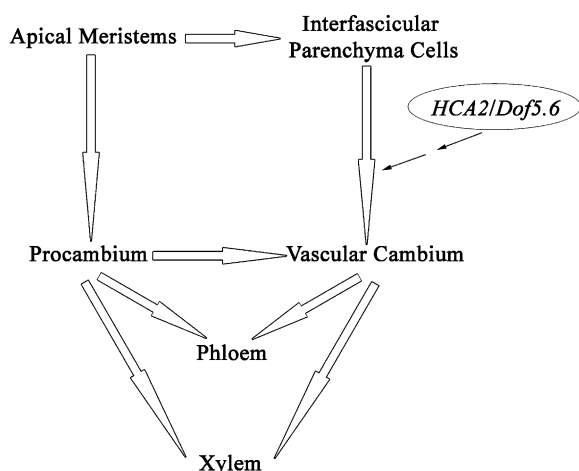
Figure 10. A Possible Model for the Role of *HCA2* during Vascular Cambium Development in *Arabidopsis.*

The diagram briefly describes the *Dof5.6/HCA2* gene involved in vascular tissue development in the inflorescence stems of *Arabidopsis*. The black and white arrows represent that one tissue generates from the other, and the thin arrow indicates that *Dof5.6/HCA2* may directly or indirectly regulate the developmental process from interfascicular parenchyma cells to vascular cambium.

showed a dramatic increase in vascular tissue development, characterized by a continuous ring of xylem/phloem, which is the consequence of premature and numerous cambium cell divisions in both the fascicular and interfascicular regions (Pineau et al., 2005). In this study, we also observed a continuous ring of vascular tissues in *hca2*. Our results suggest that the continuous ring of vascular tissues in *hca2*, perhaps in *cov1* and *hca* as well, is possibly resulting from the excess development of interfascicular cambium. In spite of the similar continuous ring of vascular tissues, *hca2* exhibited considerable differences in the organization and composition of vascular tissues compared with the other two mutants. In *cov1*, arch-shaped vascular bundles were formed, whereas in *hca*, a continuous ring of secondary tissues including xylem and phloem was formed (Parker et al., 2003; Pineau et al., 2005). In the inflorescence stems of *hca2*, however, the vascular tissues are composed of a vast amount of phloem cells, a continuous ring of cambium, and slightly restrained secondary xylem and interfascicular fibers (Figure 1D). In addition, the vascular tissues in the hypocotyls and roots of *hca2* seedlings exhibited no obvious phenotypic alterations (Figures 1L and 1N), while the diarch organization of xylem and phloem was altered in the *hca* mutant. Since *HCA2* is not allelic to *HCA* (Pineau et al., 2005) and the expression of *COV1* is not altered either in *hca2* or *HCA2* chimeric repressor plants (see Supplemental Figure 5 online), it is therefore possible that *HCA2* regulates vascular tissue development through a pathway different from those involving *HCA* and/or *COV1*. Double or triple mutant analysis will be required to test this.

A number of recently identified mutants exhibited altered patterns of vascular tissue development in inflorescence stems, with little effect in the cotyledon and leaves or vice versa (Carland et al., 1999; Deyholos et al., 2000; Koizumi et al., 2000; Parker et al., 2003; Fisher and Turner, 2007). This suggests that vascular tissue differentiation may, at least in part, be regulated by different pathways in leaves and inflorescence stems. One interesting finding of the *hca2* mutant is that high cambial activity and high phloem proliferation activity were detected not only in inflorescence stems, but also in petioles and leaf major veins, although the number and position of the major veins were not altered. This suggests that, in addition to interfascicular cambium formation/development, *HCA2* may also be involved in other developmental aspects during vascular tissue development, for instance, (pro)cambium initiation and activity. This is consistent with the hypothesis that vascular tissue development in leaves is independent of the regulation of the number and position of major veins in leaves (Dengler and Kang, 2001).

Previous studies showed that some transcription factors, including Dof proteins, have a dual function, positively and negatively regulating different target promoters (Yanagisawa, 2000, 2004; Mena et al., 2002). The number of the secondary thickened cells in the interfascicular fiber regions has been reduced, to some extent, in inflorescence stems of *hca2* (Figure 1E), possibly due to the reduced interfascicular fiber differentiation. However, the two chimeric *HCA2* repressor lines also displayed similar interfascicular fiber defects (Figures 7E and 7F). It is difficult to explain these phenomena, since *HCA2* has been shown to promote the formation of interfascicular cambium. One possible explanation is that *HCA2* may have a dual function and may also negatively regulate interfascicular fiber development. If that is the case, chimeric repression of *HCA2*, in theory, will also inactivate the downstream genes, showing the loss-of-function phenotype like the overexpression lines do. Therefore, identification of the downstream target genes of *HCA2* in different cell types may facilitate understanding of which process the *HCA2*-mediated regulatory pathway is involved in during vascular tissue development.

In conclusion, we demonstrated in this study that *Dof5.6/HCA2* positively regulates interfascicular cambium formation during vascular tissue development in *Arabidopsis* (Figure 10), which represents an important step forward in our understanding of vascular cambium formation in plants. In particular, our findings will facilitate understanding of the molecular mechanisms of interfascicular cambium formation in woody plants, which will eventually be helpful for wood quality improvement.

METHODS

Plant Material and Growth Conditions

Arabidopsis thaliana, ecotype Columbia-0, was used in experiments. Except *hca2*, all the other mutants used in this study (i.e., SALK117570, SALK008810, CS853250, SALK080292, CS873260 and CS858691) were requested from the ABRC, and the insertion sites of these mutants were confirmed by sequencing. Plants were grown on Murashige and Skoog plates (Murashige and Skoog salts [GIBCO/BRL], pH adjusted to 5.7 with 1 mol/L KOH, 0.6% [w/v] phytoagar) containing 1% sucrose or on soil in the greenhouse under long-day conditions (16-h-light/8-h-dark cycle) at 22°C ± 1°C.

hca2 was identified from a systematical screen for the mutants with vascular tissue pattern defects from the T-DNA insertion line collection in

Arabidopsis (Qin et al., 2003). Hand-cut cross sections of the base of inflorescence stems from about 2000 6-week-old plants were stained with 0.25% Toluidine blue and observed using bright-field microscopy.

TAIL-PCR and DNA Gel Blot Analyses

The flanking sequence of the T-DNA insertion was determined by TAIL-PCR with the specific and arbitrary degenerate primers as described previously (Qin et al., 2003). Genomic DNA was isolated from wild-type and *hca2* plants, and 20 μg of each sample were used for DNA gel blots as described previously (Wu et al., 2003).

Gene Cloning, Vector Construction, and Transformation

The open reading frame of *HCA2* was amplified from *Arabidopsis* cDNA by RT-PCR with primers HCA2-1 and HCA2-2. The *HCA2* promoter was amplified from *Arabidopsis* genomic DNA with primers ProHCA2-1 and ProHCA2-2. The products were cloned into the *Eco*RV site of pBluescript SK+ (pBS) in both sense (designated pBHCA2 and pBProHCA2) and antisense (designated pAHCA2 and pAProHCA2) orientations, respectively, and sequenced. 4Enhancers-*HCA2* was constructed by ligation of four DNA fragments: the *Pst*I-*Kpn*I fragment from pQG110 (Qin et al., 2005), the *Pst*I-*Sal*I enhancer tetrad fragment from pB4Ehancer (Qin et al., 2005), the *Sal*I-*Bam*HI *HCA2* promoter fragment from pAProHCA2, and the *Bam*HI-*Kpn*I *HCA2* fragment from pBHCA2.

For the RNAi constructs of *HCA2* and its homologous genes, gene-specific fragments for *HCA2* (418 bp in length), *At2g28510* (380 bp in length), *At3g45610* (330 bp in length), and *At5g60200* (276 bp in length) in the coding region, amplified with the primers for each gene, respectively (see Supplemental Table 1 online), were cloned into the *Eco*RV site of pBS in both sense and antisense orientations, respectively, and sequenced. RNAi constructs for each gene were generated by ligation of the following DNA fragments: the *Bam*HI-*Kpn*I fragment from pJim19, the *Bam*HI-*Hin*dIII fragment from each antisense-oriented pBS construct, the *Hin*dIII-*Eco*RI 1-kb GUS fragment from pBGUS (Qin et al., 2005), and the *Eco*RI-*Kpn*I fragment from each sense-oriented pBS construct.

The promoters of *ATHB8* and *SUC2* were amplified from *Arabidopsis* genomic DNA with primers ProATHB8-1, ProATHB8-2 and ProSUC2-1, ProSUC2-2 and then cloned into the *Eco*RV site of pBS in sense orientation (designated pBProATHB8 and pBProSUC2, respectively) and sequenced. The *Bam*HI-*Hin*dIII fragments of ProHCA2, ProATHB8, and ProSUC2 from pBProHCA2, pBProATHB8, and pBProSUC2 were cloned into pCAMBIA1381Xa (Cambia) digested with *Bam*HI and *Hin*dIII to fuse with the GUS reporter gene.

For the chimeric repressor construct, the coding sequence for the SRDX repression domain (LDLDLELRLGFA) (Hiratsu et al., 2002, 2003, 2004) containing an *Spe*I enzyme site (SRDX-1) and that for the antisense sequence containing an *Nhe*I enzyme site (SRDX-2) were mixed and annealed and digested with these two restriction enzymes before it was cloned into pCAMBIA1390 (Cambia) digested with the same two restriction enzymes (designated pCSRDX) and sequence confirmed. The coding sequence of *HCA2* (without the stop codon) was amplified from *Arabidopsis* cDNA by RT-PCR with primers HCA2-1 and HCA2NS, cloned into the *Eco*RV site of pBS, and sequence screened for the clone with the gene in sense orientation (designated pBHCA2NS). *35S: HCA2SRDX* was constructed by the ligation of three DNA fragments: the *Pst*I-*Spe*I fragment from pCSRDX, the *Pst*I-*Kpn*I 35S promoter fragment from pQG110, and the *Kpn*I-*Spe*I *HCA2* fragment from pBHCA2NS. *ProHCA2: HCA2SRDX* was constructed by ligation of three DNA fragments: the *Pst*I-*Spe*I fragment from pCSRDX, the *Pst*I-*Kpn*I fragment from pBProHCA2, and the *Kpn*I-*Spe*I *HCA2* fragment from pBHCA2NS.

Constructs were transformed into *Agrobacterium tumefaciens* GV3101/pMP90, using a freeze-thaw procedure. *Arabidopsis* transformation and transgenic plant screening were conducted as previously reported (Qin et al., 2005).

RNA Extraction and Reverse Transcription

Total RNA from the frozen material was extracted using TRIzol reagent. To eliminate the contamination of genomic DNA, total RNA was then treated with RNase-free DNase (TaKaRa). Five micrograms of total RNA was reverse transcribed using the Superscript II RT kit (Invitrogen) in a reaction of 20 μL. The cDNA was diluted 50 times and later used as the template for RT-PCR or quantitative RT-PCR as previously described (Liu et al., 2008).

Quantitative Real-Time RT-PCR

The PCR amplification was performed on an MJ Research thermocycler, using a DyNAmo SYBR Green qPCR kit (Finnzymes) and the protocol as previously described (Xing et al., 2007). Each reaction was performed on 2 μL diluted cDNA sample, in a total reaction system of 10 μL. The procedure of the reaction was set according to the manufacturer's protocol, and sequences of primers used in this work are shown in Supplemental Table 1 online. To check the specificity of amplification, the melting curve of the PCR products was detected. The expression levels of different genes were standardized to the constitutive expression level of *UBQ10*. In one quantitative RT-PCR experiment, at least three values were produced for each sample. The relative expression level of each gene, corresponding to the expression level of *UBQ10*, was calculated using $2^{-\Delta\Delta t}$ method (Livak and Schmittgen, 2001).

Microscopy

Different portions of inflorescences stems from wild-type, mutant, and transgenic plants were collected and fixed in FAA solution (50% ethanol, 5% acetic acid, and 3.7% formaldehyde). After dehydration through a concentration-increasing ethanol series, the samples were embedded into Historesin (Leica). Sectioning was performed using a Leica microtome and the sections mounted on slides. Sections of 7 μm were stained with 0.25% (w/v) Toluidine blue O (Sigma-Aldrich) or safranin and observed under an Olympus BX51 microscope as described by Qin et al. (2007). Hand-cut sections from fresh *Arabidopsis* stems were stained with 0.1% Aniline blue and observed using an Olympus BX51 microscope, equipped with epifluorescence illumination (excitation filter bandpass 340 to 380 nm; suppression filter LP 430 nm). Digital images were captured with a SPOT camera (Diagnostic Instruments) and processed using Adobe Photoshop.

For scanning electron microscopy, mature inflorescence stems and the fifth true leaves of wild-type and mutant plants were fixed in FAA solution for at least 24 h and then transferred to 95% ethanol overnight. The chosen specimens were dehydrated in the following ethanol and isoamyl acetate series: 95% ethanol, 100% ethanol, 75% ethanol + 25% isoamyl acetate, 50% ethanol + 50% isoamyl acetate, 25% ethanol + 75% isoamyl acetate, and 100% isoamyl acetate. The specimens were CO_2 critical point dried and coated with gold for scanning electron microscopy observation as described by Zhang et al. (2007).

Measurement of Leaf Index

Arabidopsis plants were grown under long-day conditions. Images of more than 15 fifth true leaves of 6-week-old *Arabidopsis* plants were captured using a digital camera. The length of leaf blades was measured using ImageJ software (http://rsb.info.nih.gov/ij/), and then the mean value was calculated for each measurement.

Nuclear Localization Analysis

The *YFP* gene with or without a stop codon was amplified from pIRES-YFP (CLONTECH) with primers YFP-1 and YFP-2 or primers YFP-1 and YFPNS. The *YFP* fragment with stop codon was cloned into the *Eco*RV site of pBS in sense orientation (designated pBYFP) and that without stop codon in antisense orientation (designated pAYFPNS). *35S:YFP-HCA2* was constructed by ligation of three DNA fragments: the *Kpn*I-*Sal*I fragment from pQG110 (Qin et al., 2005), the *Kpn*I-*Bam*HI fragment from pAYFPNS, and the *Bam*HI-*Sal*I *HCA2* fragment from pBHCA2. *35S: YFP* was constructed by the ligation of the *Bam*HI/*Kpn*I-digested fragment from pBYFP and *Bam*HI/*Kpn*I -digested vector pQG110. The nuclear localization assay was conducted as described previously (Yi et al., 2002).

Transactivation Activity Assays

Full-length coding region and various deletion mutants of *HCA2* were amplified by PCR using *Pfu* DNA polymerase. The products were cloned into the *Eco*RV site of pBS in sense orientation and sequenced. Inserts were fused in frame to the sequences encoding the GAL4 DNA binding domain by cloning them into *Eco*RI/*Sal*I sites of pYF503 (Ye et al., 2004). Yeast strain EGY48, and the reporter vector pG221, which harbors the *CYC1* core promoter and β-galactosidase (LacZ) reporter gene, were used for this assay (Li et al., 2006). Yeast LiAc-mediated transformations and β-galactosidase filter assays using X-gal were performed as described in the Clonetech Yeast Protocols Handbook. Yeast transformants were screened on the synthetic dropout SD/-Ura and SD/-Ura/-Trp medium.

Assays of GUS Activity

The histochemical GUS assay was performed in a staining solution containing 0.5 mg/mL 5-bromo-4-chloro-3-indolyl glucuronide in 0.1 M Na_2HPO_4, pH 7.0, 10 mM Na_2EDTA, 0.5 mM potassium ferricyanide/ferrocyanide, and 0.06% Triton X-100 (Jefferson et al., 1987). Samples were infiltrated under vacuum for 10 min and then incubated at 37°C overnight. The staining buffer was removed, and the samples were cleared in 70% ethanol. All observations by light microscopy were made with the Olympus BX51 microscope system.

Accession Numbers

Sequence data from this article can be found in the Arabidopsis Genome Initiative or GenBank/EMBL databases under the following accession numbers: *Dof5.6/HCA2* (*At5g62940*), *ATHB8* (*At4g32880*), *SUC2* (*At1g22710*), *APL* (*At1g79430*), *RTM1* (*At1g05760*), *AHA3* (*At5g57350*), *ANT* (*At4g37750*), *EXPA9* (*At5g02260*), *IRX1* (*At4g18780*), *IRX5* (*At5g44030*), and *COV1* (*At2g20120*).

Supplemental Data

The following materials are available in the online version of this article.

Supplemental Figure 1. The Expression Level of *HCA2* and *At5g60200* Was Not Altered in Their Corresponding SALK Mutants.

Supplemental Figure 2. RNAi Transgenic Lines of *HCA2* and Its Homologous Genes Did Not Display Obvious Vascular Tissue-Associated Phenotypes.

Supplemental Figure 3. The Expression of *HCA2* and One of Its Homologous Genes Was Reduced in One *HCA2* RNAi Transgenic Line.

Supplemental Figure 4. *HCA2* and Its Homologous Genes Were All Downregulated in the Double RNAi Transgenic Line and Led to No Obvious Phenotype.

Supplemental Figure 5. *COV1* Is Not Regulated by *HCA2*

Supplemental Table 1. Primer Information for Genes Used in This Study.

REFERENCES

Altamura, M.M., Possenti, M., Matteucci, A., Baima, S., Ruberti, I., and Morelli, G. (2001). Development of the vascular system in the inflorescence stem of *Arabidopsis.* New Phytol. **151:** 381–389.

Baima, S., Nobili, F., Sessa, G., Lucchetti, S., Ruberti, I., and Morelli, G. (1995). The expression of the *Athb-8* homeobox gene is restricted to provascular cells in *Arabidopsis thaliana.* Development **121:** 4171–4182.

Baima, S., Possenti, M., Matteucci, A., Wisman, E., Altamura, M.M., Ruberti, I., and Morelli, G. (2001). The *Arabidopsis* ATHB-8 HD-zip protein acts as a differentiation-promoting transcription factor of the vascular meristems. Plant Physiol. **126:** 643–655.

Baucher, M., El Jaziri, M., and Vandeputte, O. (2007). From primary to secondary growth: Origin and development of the vascular system. J. Exp. Bot. **58:** 3485–3501.

Bonke, M., Thitamadee, S., Mahonen, A.P., Hauser, M.T., and Helariutta, Y. (2003). *APL* regulates vascular tissue identity in *Arabidopsis.* Nature **426:** 181–186.

Carland, F.M., Berg, B.L., FitzGerald, J.N., Jinamornphongs, S., Nelson, T., and Keith, B. (1999). Genetic regulation of vascular tissue patterning in *Arabidopsis.* Plant Cell **11:** 2123–2137.

Carlsbecker, A., and Helariutta, Y. (2005). Phloem and xylem specification: pieces of the puzzle emerge. Curr. Opin. Plant Biol. **8:** 512–517.

Chisholm, S.T., Parra, M.A., Anderberg, R.J., and Carrington, J.C. (2001). *Arabidopsis RTM1* and *RTM2* genes function in phloem to restrict long-distance movement of tobacco etch virus. Plant Physiol. **127:** 1667–1675.

Dengler, N., and Kang, J. (2001). Vascular patterning and leaf shape. Curr. Opin. Plant Biol. **4:** 50–56.

Dewitt, N.D., and Sussman, M.R. (1995). Immunocytological localization of an epitope-tagged plasma membrane proton pump (H+-ATPase) in phloem companion cells. Plant Cell **7:** 2053–2067.

Deyholos, M.K., Cordner, G., Beebe, D., and Sieburth, L.E. (2000). The *SCARFACE* gene is required for cotyledon and leaf vein patterning. Development **127:** 3205–3213.

Emery, J.F., Floyd, S.K., Alvarez, J., Eshed, Y., Hawker, N.P., Izhaki, A., Baum, S.F., and Bowman, J.L. (2003). Radial patterning of *Arabidopsis* shoots by class III *HD-ZIP* and *KANADI* genes. Curr. Biol. **13:** 1768–1774.

Esau, K. (1977). Anatomy of Seed Plants. (New York: Wiley).

Fisher, K., and Turner, S. (2007). PXY, a receptor-like kinase essential for maintaining polarity during plant vascular-tissue development. Curr. Biol. **17:** 1061–1066.

Fukuda, H. (2004). Signals that control plant vascular cell differentiation. Nat. Rev. Mol. Cell Biol. **5:** 379–391.

Gray-Mitsumune, M., Mellerowicz, E.J., Abe, H., Schrader, J., Winzell, A., Sterky, F., Blomqvist, K., McQueen-Mason, S., Teeri, T.T., and Sundberg, B. (2004). Expansins abundant in secondary xylem belong to subgroup A of the alpha-expansin gene family. Plant Physiol. **135:** 1552–1564.

Groover, A.T., Mansfield, S.D., DiFazio, S.P., Dupper, G., Fontana, J.R., Millar, R., and Wang, Y. (2006). The *Populus* homeobox gene *ARBORKNOX1* reveals overlapping mechanisms regulating the shoot apical meristem and the vascular cambium. Plant Mol. Biol. **61:** 917–932.

Gualberti, G., Papi, M., Bellucci, L., Ricci, I., Bouchez, D., Camilleri, C., Costantino, P., and Vittorioso, P. (2002). Mutations in the Dof zinc finger genes *DAG2* and *DAG1* influence with opposite effects the germination of *Arabidopsis* seeds. Plant Cell **14:** 1253–1263.

Hanzawa, Y., Takahashi, T., and Komeda, Y. (1997). *ACL5*: An *Arabidopsis* gene required for internodal elongation after flowering. Plant J. **12:** 863–874.

Helariutta, Y. (2007). Cell signalling during vascular morphogenesis. Biochem. Soc. Trans. **35:** 152–155.

Hiratsu, K., Matsui, K., Koyama, T., and Ohme-Takagi, M. (2003). Dominant repression of target genes by chimeric repressors that include the EAR motif, a repression domain, in *Arabidopsis.* Plant J. **34:** 733–739.

Hiratsu, K., Mitsuda, N., Matsui, K., and Ohme-Takagi, M. (2004). Identification of the minimal repression domain of SUPERMAN shows that the DLELRL hexapeptide is both necessary and sufficient for repression of transcription in *Arabidopsis.* Biochem. Biophys. Res. Commun. **321:** 172–178.

Hiratsu, K., Ohta, M., Matsui, K., and Ohme-Takagi, M. (2002). The SUPERMAN protein is an active repressor whose carboxy-terminal repression domain is required for the development of normal flowers. FEBS Lett. **514:** 351–354.

Hou, H.-W., Zhou, Y.-T., Mwange, K.-N.K., Li, W.-F., He, X.-Q., and Cui, K.-M. (2006). *ABP1* expression regulated by IAA and ABA is associated with the cambium periodicity in *Eucommia ulmoides* Oliv. J. Exp. Bot. **57:** 3857–3867.

Iqbal, M., and Ghouse, A.K.M. (1990). Cambial concept and organization. In The Vascular Cambium, M. Iqbal, ed (Taunton, UK: Research Studies Press), pp. 1–36.

Ito, Y., Nakanomyo, I., Motose, H., Iwamoto, K., Sawa, S., Dohmae, N., and Fukuda, H. (2006). Dodeca-CLE peptides as suppressors of plant stem cell differentiation. Science **313:** 842–845.

Jefferson, R.A., Kavanagh, T.A., and Bevan, M.W. (1987). GUS fusions: *Beta-glucuronidase* as a sensitive and versatile gene fusion marker in higher plants. EMBO J. **6:** 3901–3907.

Johansson, A.-M., Wang, C., Stenberg, A., Hertzberg, M., Little, C.H.A., and Olsson, O. (2003). Characterization of a *PttRPS18* promoter active in the vascular cambium region of hybrid aspen. Plant Mol. Biol. **52:** 317–329.

Ko, J.-H., Prassinos, C., and Han, K.-H. (2006). Developmental and seasonal expression of *PtaHB1*, a *Populus* gene encoding a class III HD-Zip protein, is closely associated with secondary growth and inversely correlated with the level of microRNA (miR166). New Phytol. **169:** 469–478.

Koizumi, K., Sugiyama, M., and Fukuda, H. (2000). A series of novel mutants of *Arabidopsis thaliana* that are defective in the formation of continuous vascular network: Calling the auxin signal flow canalization hypothesis into question. Development **127:** 3197–3204.

Konishi, M., and Yanagisawa, S. (2007). Sequential activation of two Dof transcription factor gene promoters during vascular development in *Arabidopsis thaliana.* Plant Physiol. Biochem. **45:** 623–629.

Kozlowski, T.T., and Pallardy, S.G. (1997). Physiology of Woody Plants. (San Diego, CA: Academic Press).

Lachaud, S., Catesson, A.M., and Bonnemain, J.L. (1999). Structure and functions of the vascular cambium. C. R. Acad. Sci. III **322:** 633–650.

Larson, P.R. (1994). The Vascular Cambium: Development and Structure. (Berlin: Springer).

Lev-Yadun, S., and Flaishman, M.A. (2001). The effect of submergence on ontogeny of cambium and secondary xylem and on fiber lignifications in inflorescence stems of *Arabidopsis.* IAWA J. **22:** 159–169.

Li, J., Yang, X., Wang, Y., Li, X., Gao, Z., Pei, M., Chen, Z., Qu, L.-J., and Gu, H. (2006). Two groups of MYB transcription factors share a motif which enhances trans-activation activity. Biochem. Biophys. Res. Commun. **341:** 1155–1163.

Lijavetzky, D., Carbonero, P., and Vicente-Carbajosa, J. (2003). Genome-wide comparative phylogenetic analysis of the rice and *Arabidopsis* Dof gene families. BMC Evol. Biol. **3:** 1–11.

Little, C.H.A., MacDonald, J.E., and Olssont, O. (2002). Involvement of indole-3-acetic acid in fascicular and interfascicular cambial growth and interfascicular extraxylary fiber differentiation in *Arabidopsis thaliana* inflorescence stems. Int. J. Plant Sci. **163:** 519–529.

Liu, J., et al. (2008). Targeted degradation of the cyclin-dependent kinase inhibitor ICK4/KRP6 by RING-type E3 ligases is essential for mitotic cell cycle progression during *Arabidopsis* gametogenesis. Plant Cell **20:** 1538–1554.

Livak, K.J., and Schmittgen, T.D. (2001). Analysis of relative gene expression data using real-time quantitative PCR and the 2(-Delta Delta C(T)) Method. Methods **25:** 402–408.

Mauseth, J.D. (1988). Plant Anatomy. (Menlo Park, CA: Benjamin/Cummings).

McConnell, J.R., Emery, J., Eshed, Y., Bao, N., Bowman, J., and Barton, M.K. (2001). Role of *PHABULOSA* and *PHAVOLUTA* in determining radial patterning in shoots. Nature **411:** 709–713.

Mellerowicz, E.J., Baucher, M., Sundberg, B., and Boerjan, W. (2001). Unravelling cell wall formation in the woody dicot stem. Plant Mol. Biol. **47:** 239–274.

Mena, M., Cejudo, F.J., Isabel-Lamoneda, I., and Carbonero, P. (2002). A role for the DOF transcription factor BPBF in the regulation of gibberellin-responsive genes in barley aleurone. Plant Physiol. **130:** 111–119.

Mena, M., Vicente-Carbajosa, J., Schmidt, R.J., and Carbonero, P. (1998). An endosperm-specific DOF protein from barley, highly conserved in wheat, binds to and activates transcription from the prolamin-box of a native B-hordein promoter in barley endosperm. Plant J. **16:** 53–62.

Mitsuda, N., Iwase, A., Yamamoto, H., Yoshida, M., Seki, M., Shinozaki, K., and Ohme-Takagi, M. (2007). NAC transcription factors, NST1 and NST3, are key regulators of the formation of secondary walls in woody tissues of *Arabidopsis.* Plant Cell **19:** 270–280.

Motose, H., Sugiyama, M., and Fukuda, H. (2004). A proteoglycan mediates inductive interaction during plant vascular development. Nature **429:** 873–878.

Papi, M., Sabatini, S., Bouchez, D., Camilleri, C., Costantino, P., and Vittorioso, P. (2000). Identification and disruption of an *Arabidopsis* zinc finger gene controlling seed germination. Genes Dev. **14:** 28–33.

Park, D.H., Lim, P.O., Kim, J.S., Cho, D.S., Hong, S.H., and Nam, H.G. (2003). The *Arabidopsis COG1* gene encodes a Dof domain transcription factor and negatively regulates phytochrome signaling. Plant J. **34:** 161–171.

Parker, G., Schofield, R., Sundberg, B., and Turner, S. (2003). Isolation of *COV1*, a gene involved in the regulation of vascular patterning in the stem of *Arabidopsis.* Development **130:** 2139–2148.

Pineau, C., et al. (2005). *hca*: An *Arabidopsis* mutant exhibiting unusual cambial activity and altered vascular patterning. Plant J. **44:** 271–289.

Plesch, G., Ehrhardt, T., and Mueller-Roeber, B. (2001). Involvement of TAAAG elements suggests a role for Dof transcription factors in guard cell-specific gene expression. Plant J. **28:** 455–464.

Qin, G., Ma, Z., Zhang, L., Xing, S., Hou, X., Deng, J., Liu, J., Chen, Z., Qu, L.-J., and Gu, H. (2007). *Arabidopsis AtBECLIN 1/AtAtg6/AtVps30* is essential for pollen germination and plant development. Cell Res. **17:** 249–263.

Qin, G., Gu, H., Zhao, Y., Ma, Z., Shi, G., Yang, Y., Pichersky, E., Chen, H., Liu, M., Chen, Z., and Qu, L.-J. (2005). An indole-3-acetic acid carboxyl methyltransferase regulates *Arabidopsis* leaf development. Plant Cell **17:** 2693–2704.

Qin, G., et al. (2003). Obtaining and analysis of flanking sequences from T-DNA transformants of *Arabidopsis.* Plant Sci. **165:** 941–949.

Ratcliffe, O.J., Riechmann, J.L., and Zhang, J.Z. (2000). *INTERFASCICULAR FIBERLESS1* is the same gene as *REVOLUTA.* Plant Cell **12:** 315–317.

Sauer, N., and Stolz, J. (1994). SUC1 and SUC2: Two sucrose transporters from *Arabidopsis thaliana*; expression and characterization in baker's yeast and identification of the histidine-tagged protein. Plant J. **6:** 67–77.

Savidge, R.A. (1996). Xylogenesis, genetic and environmental regulation: A review. IAWA J. **17:** 269–310.

Scarpella, E., and Meijer, A.H. (2004). Pattern formation in the vascular system of monocot and dicot plant species. New Phytol. **164:** 209–242.

Schrader, J., Nilsson, J., Mellerowicz, E., Berglund, A., Nilsson, P., Hertzberg, M., and Sandberg, G. (2004). A high-resolution transcript profile across the wood-forming meristem of poplar identifies potential regulators of cambial stem cell identity. Plant Cell **16:** 2278–2292.

Sieburth, L.E., and Deyholos, M.K. (2006). Vascular development: The long and winding road. Curr. Opin. Plant Biol. **9:** 48–54.

Skirycz, A., Jozefczuk, S., Stobiecki, M., Muth, D., Zanor, M.I., Witt, I., and Mueller-Roeber, B. (2007). Transcription factor AtDOF4;2 affects phenylpropanoid metabolism in *Arabidopsis thaliana.* New Phytol. **175:** 425–438.

Skirycz, A., Reichelt, M., Burow, M., Birkemeyer, C., Rolcik, J., Kopka, J., Zanor, M.I., Gershenzon, J., Strnad, M., Szopa, J., Mueller-Roeber, B., and Witt, I. (2006). DOF transcription factor AtDof1.1 (OBP2) is part of a regulatory network controlling glucosinolate biosynthesis in *Arabidopsis.* Plant J. **47:** 10–24.

Stadler, R., and Sauer, N. (1996). The *Arabidopsis thaliana AtSUC2* gene is specifically expressed in companion cells. Bot. Acta **109:** 299–306.

Taylor, N.G., Howells, R.M., Huttly, A.K., Vickers, K., and Turner, S.R. (2003). Interactions among three distinct CesA proteins essential for cellulose synthesis. Proc. Natl. Acad. Sci. USA **100:** 1450–1455.

van Raemdonck, D., Pesquet, E., Cloquet, S., Beeckman, H., Boerjan, W., Goffner, D., El Jaziri, M., and Baucher, M. (2005). Molecular changes associated with the setting up of secondary growth in aspen. J. Exp. Bot. **56:** 2211–2227.

Vicente-Carbajosa, J., Moose, S.P., Parsons, R.L., and Schmidt, R.J. (1997). A maize zinc-finger protein binds the prolamin box in zein gene promoters and interacts with the basic leucine zipper transcriptional activator Opaque2. Proc. Natl. Acad. Sci. USA **94:** 7685–7690.

Wu, L., Fan, Z., Guo, L., Li, Y., Zhang, W., Gu, H., Jacobs, M., Qu, L.-J., and Chen, Z. (2003). Over-expression of an *Arabidopsis δ-OAT* gene enhances salt and drought tolerance in transgenic rice. Chin. Sci. Bull. **48:** 2594–2600.

Xing, S., Qin, G., Shi, Y., Ma, Z., Chen, Z., Gu, H., and Qu, L.-J. (2007). *GAMT2* encodes a methyltransferase of gibberellic acid that is involved in seed maturation and germination in *Arabidopsis.* J. Integr. Plant Biol. **49:** 368–381.

Yanagisawa, S. (2000). Dof1 and Dof2 transcription factors are associated with expression of multiple genes involved in carbon metabolism in maize. Plant J. **21:** 281–288.

Yanagisawa, S. (2002). The Dof family of plant transcription factors. Trends Plant Sci. **7:** 555–560.

Yanagisawa, S. (2004). Dof domain proteins: Plant-specific transcription factors associated with diverse phenomena unique to plants. Plant Cell Physiol. **45:** 386–391.

Yanagisawa, S., and Sheen, J. (1998). Involvement of maize Dof zinc finger proteins in tissue-specific and light-regulated gene expression. Plant Cell **10:** 75–89.

Yang, X., Tuskan, G.A., and Cheng, M.Z. (2006). Divergence of the Dof gene families in poplar, *Arabidopsis*, and rice suggests multiple modes of gene evolution after duplication. Plant Physiol. **142:** 820–830.

Ye, R., Yao, Q.-H., Xu, Z.-H., and Xue, H.-W. (2004). Development of an efficient method for the isolation of factors involved in gene transcription during rice embryo development. Plant J. **38:** 348–357.

Yi, L., Qu, L.-J., Chang, S., Su, Y., Gu, H., and Chen, Z. (2002). Two nuclear localization signals required for the nuclear localization of rice ribosomal protein S4. Plant Sci. **162:** 251–256.

Zhang, X., Chen, Y., Wang, Z.-Y., Chen, Z., Gu, H., and Qu, L.-J. (2007). Constitutive expression of *CIR1* (*RVE2*) affects several circadian-regulated processes and seed germination in *Arabidopsis.* Plant J. **51:** 512–525.

Zhao, C., Craig, J.C., Petzold, H.E., Dickerman, A.W., and Beers, E.P. (2005). The xylem and phloem transcriptomes from secondary tissues of the *Arabidopsis* root-hypocotyl. Plant Physiol. **138:** 803–818.

Zhong, R., Lee, C., Zhou, J., McCarthy, R.L., and Ye, Z.-H. (2008). A battery of transcription factors involved in the regulation of secondary cell wall biosynthesis in *Arabidopsis.* Plant Cell **20:** 2763–2782.

Zhong, R., Richardson, E.A., and Ye, Z.-H. (2007). Two NAC domain transcription factors, SND1 and NST1, function redundantly in regulation of secondary wall synthesis in fibers of *Arabidopsis.* Planta **225:** 1603–1611.

Zhong, R., Taylor, J.J., and Ye, Z.-H. (1997). Disruption of interfascicular fiber differentiation in an *Arabidopsis* mutant. Plant Cell **9:** 2159–2170.

Zhong, R., and Ye, Z.-H. (1999). *IFL1*, a gene regulating interfascicular fiber differentiation in *Arabidopsis*, encodes a homeodomain-leucine zipper protein. Plant Cell **11:** 2139–2152.